

Sierpinski-Carpet Fractal Frequency Reconfigurable Microstrip Patch Antenna Design for Ku/K/Ka Band Application

Iqra Masroor*, Jamshed A. Ansari, Shadman Aslam, and Abhishek K. Saroj

Abstract—This work discusses the effect of reconfigurability on a Sierpinski-carpet fractal microstrip patch antenna. The implementation of reconfigurability is achieved by modeling a PIN diode as a lumped RC element on HFSS (High Frequency Structure Simulator) simulation tool. The proposed antenna design is also fabricated and tested. It is highly miniaturized having a dimension of $9.5\text{ mm} \times 7.4\text{ mm}$ and a significantly high impedance bandwidth which is desirable for most wireless communication applications. The resultant Fractal Reconfigurable Antenna (FRA) exhibits good performance parameters having frequency reconfigurability rendering it useful for Ku/K/Ka band applications.

1. INTRODUCTION

Amongst a wide variety of antennas, microstrip patch antennas have become quite popular in the recent decades. Their inexpensive design, low profile, mechanical ruggedness, and conformable shape are some of the key reasons for their success [1]. Consequently, the research for novel microstrip patch antennas has also gained momentum. Different design approaches have been introduced and aspects discovered to improve the antenna performance parameters; primarily, impedance bandwidth, gain, and radiation efficiency.

The goal to achieve size-compactness and multiband/wideband response can be attained by the exploitation of fractal geometries in antennas [2]. Various fractals such as Koch curve, Hilbert curve, Sierpinski and Minkowski fractals have been investigated and implemented in recent years. In [3], the Sierpinski carpet fractal geometry has been employed for a microstrip antenna array enabling dual-band operation. Modification of the antenna properties can also be obtained by the use of various reconfiguration techniques [4]. Reconfigurable antennas provide a dynamic response by the redistribution of the RF currents over the antenna surface. An interesting subject would be now to explore a merger of fractal and reconfigurable antennas. An effective insight on fractal antenna engineering, reconfigurable antennas and the combination of fractal-shapes with electronic reconfigurability is presented in [5].

Reconfigurability can be achieved in terms of antenna polarization, frequency, radiation pattern, or a combination of these [6]. Switching components like MEMs, varactor diodes, and PIN diodes are some elements that can be used for reconfigurability [7, 8]. The introduction of fractal geometries in reconfigurable antennas further facilitates performance improvement. The use of fractal geometry as an antenna size-reduction technique has been used extensively in recent times [9]. In [10–12], frequency reconfigurability is achieved by the introduction of PIN diodes as switching elements in the conventional patch antenna. Interesting and novel designs of frequency reconfigurable antennas capable of switching among four frequency bands are proposed in [13] and [14] providing multifunction operation. Polarization reconfigurable antennas also have an important role in several applications like

Received 20 September 2021, Accepted 27 November 2021, Scheduled 3 December 2021

* Corresponding author: Iqra Masroor (iqraec1029@gmail.com).

The authors are with the Department of Electronics & Communication, University of Allahabad, Prayagraj, India.

remote sensing, tracking, and guiding owing to their ability to avoid fading losses [15]. One of the most challenging areas of antenna reconfigurability is to realize reconfigurable radiation patterns [16].

Multiple services are provided to the end devices by frequency reconfigurable antennas and other advantages in terms of compact size, radiation pattern and gain [17]. The generation of about nine frequency bands has been achieved by employing only six PIN diodes resulting in frequency reconfigurability in [18]. In the proposed work, an illustrative design of a frequency reconfigurable fractal microstrip patch antenna has been presented and discussed, and the effect of diode ON/OFF states has been observed. The fractal geometry employed is a Sierpinski carpet fractal up to 2 iterations. This geometry can be easily incorporated in conventional microstrip antenna designs for obtaining multiband/wideband operations and/or size-reduction and has been used for a variety of applications such as 5G commercial applications [19] and UWB applications [20].

2. DESIGN COMPOSITION AND METHODOLOGY

2.1. Antenna Design Flow

A simple design flow for the formation of proposed Fractal Reconfigurable Antenna (FRA) is illustrated in Fig. 1. The design of a conventional microstrip patch antenna [21], followed by optimization of

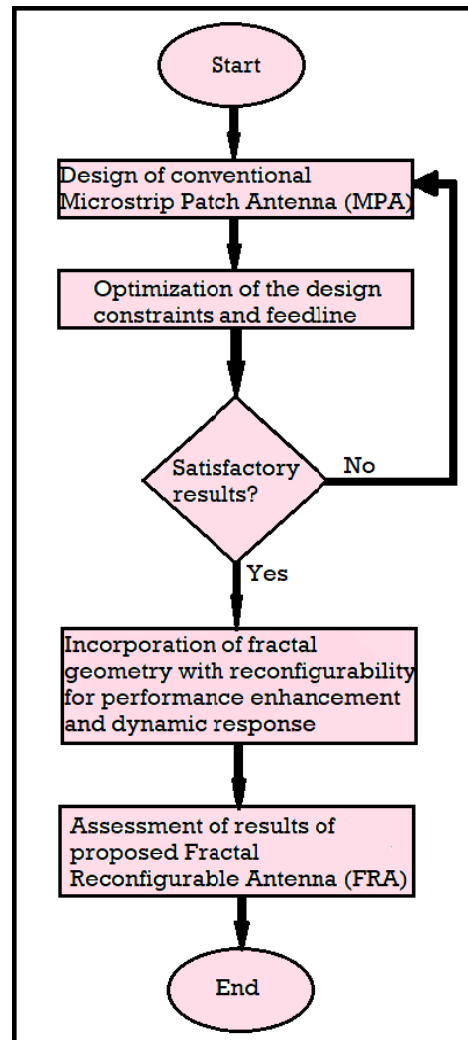


Figure 1. Proposed antenna design flow.

the design constraints to meet requirements and successive implementation of fractal geometry with reconfigurability are the key steps of the design. The design frequency (f) chosen is 15 GHz such that the desired antenna frequency range lies in the Ku-band (12–18 GHz). The following section discusses the formation of Sierpinski-carpet fractal geometry, modeling of the PIN diode, and resultant design model of the proposed FRA.

2.2. Sierpinski-Carpet Fractal Geometry

Fractals are self-similar geometries exhibiting Hausdorff dimension described by a power law equation:

$$X = S^D \quad (1)$$

where S is the scaling factor, and X is the largest number of non-empty self-similar copies. Taking natural logarithm on both the sides of Equation (1), we get

$$D = \frac{\ln X}{\ln S} \quad (2)$$

which is known as the Hausdorff dimension [22].

Waclaw Sierpinski, in 1916, described Sierpinski carpet as a plane fractal, whose construction starts from a square. The Sierpinski carpet fractal is a deterministic fractal that can be simply constructed using square geometries by an iterative process [23]. The initial square is divided into 9 sub-squares, each having the same shape and size, and the central sub-square is eliminated. Recursively applying this process to the remaining 8 sub-squares, for i iterations, where i may tend to infinity, generates the Sierpinski carpet fractal. For the proposed antenna design, Sierpinski-carpet fractal for 2 iterations has been exploited. A measure of the fractal dimension is the Hausdorff dimension (D), also known as the topological dimension. For Sierpinski carpet fractal, the scaling factor (S) is 3, and the mass ratio (X) is 8, as shown in Fig. 2. Therefore, the Hausdorff dimension (D) is given by:

$$D = \frac{\ln X}{\ln S} = \frac{\log 8}{\log 3} = 1.8928$$

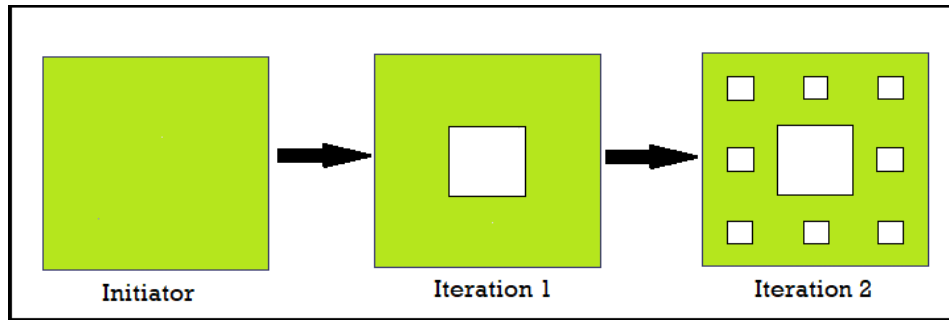


Figure 2. Sierpinski-carpet fractal geometry for 2 iterations.

2.3. Modeling of PIN Diode as Lumped RC Element

A single PIN diode is modeled as a lumped RC element in HFSS for incorporating reconfigurability in the fractal microstrip patch antenna [24]. Assuming the PIN diode to behave as a short circuit in the conducting mode and as an open circuit in the non-conducting mode, the ON/OFF state of the diode is obtained. The technical datasheet of MA4SPS402 PIN diode has been utilized for diode modeling [25]. In the modeling of PIN diode, the effect of parasitic inductance has been neglected because being a surface mount diode, it has a very low value of parasitic inductance, i.e., 0.45 nH, which can be ignored in the simulation. The On-state resistance (R_1) has been taken as 5 ohm while the Off-state resistance (R_2) and capacitance (C) chosen are 40 kohm and 0.03 pF, respectively. The RC equivalent circuit of the PIN diode is as shown in Fig. 3.

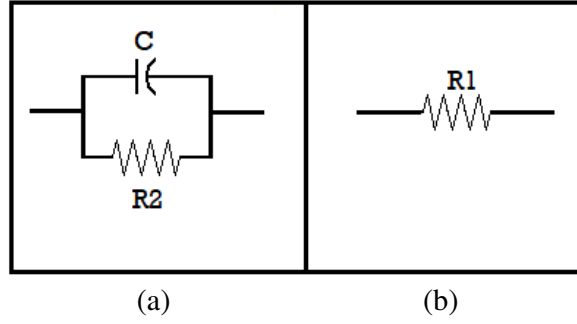


Figure 3. Equivalent circuit of PIN diode (a) off-state, (b) on-state [$R1 = 5 \text{ ohm}$, $R2 = 40 \text{ kohm}$ and $C = 0.03 \text{ pF}$].

2.4. Proposed FRA Design Model

Figure 4 illustrates the design model of the proposed FRA, showing the top-view, bottom-view, and side-view, respectively. FR4-epoxy substrate material is used with the given specifications:

- Relative permittivity: $\epsilon_r = 4.4$
- Dielectric loss tangent: $\delta = 0.02$
- Substrate thickness: $h = 1.6 \text{ mm}$

Microstrip antennas with rectangular or square patches can be simply modeled as sections of transmission lines, and the transmission line model can be used to analyze a rectangular microstrip patch antenna. The dimensions of the conventional microstrip patch antenna have been evaluated using the mathematical equations below [26]:

The patch-width (w_p) is given by:

$$w_p = \frac{c}{2f} \sqrt{\frac{2}{\epsilon_r + 1}} \quad (3)$$

where c is the velocity of light, f the design frequency, and ϵ_r the relative permittivity of the substrate.

The patch-length (l_P) is given by:

$$l_P = l_{ef} - 2\Delta l \quad (4a)$$

where l_{ef} is the effective length of the patch:

$$l_{ef} = \frac{c}{2f\sqrt{\epsilon_{ref}}} \quad (4b)$$

where ϵ_{ref} is the effective dielectric constant of substrate:

$$\epsilon_{ref} = \frac{\epsilon_r + 1}{2} + \frac{\epsilon_r - 1}{2} \left[1 + \frac{12h}{w_p} \right]^{-1/2} \quad (4c)$$

The normalized extension in length (Δl) is given by:

$$\Delta l = 0.412h \frac{(\epsilon_{ref} + 0.3) \left(\frac{w_p}{h} + 0.264 \right)}{(\epsilon_{ref} - 0.258) \left(\frac{w_p}{h} + 0.8 \right)} \quad (4d)$$

The cavity model can also be used for the theoretical study of microstrip patch antennas [27, 28]. The dimensions of the proposed antenna are $9.5 \text{ mm} \times 7.4 \text{ mm}$ for the ground plane and $6 \text{ mm} \times 3.9 \text{ mm}$ for the patch, making the antenna compact. A portion of the patch has been fractaled with Sierpinski carpet of dimension $1.8 \text{ mm} \times 1.8 \text{ mm}$, and it is connected to the remaining patch by inclusion of the PIN diode. Microstrip line feed is used to provide excitation to the patch. It is easy to model since it is simply an extension of the patch itself, and the feedline width has been optimized.

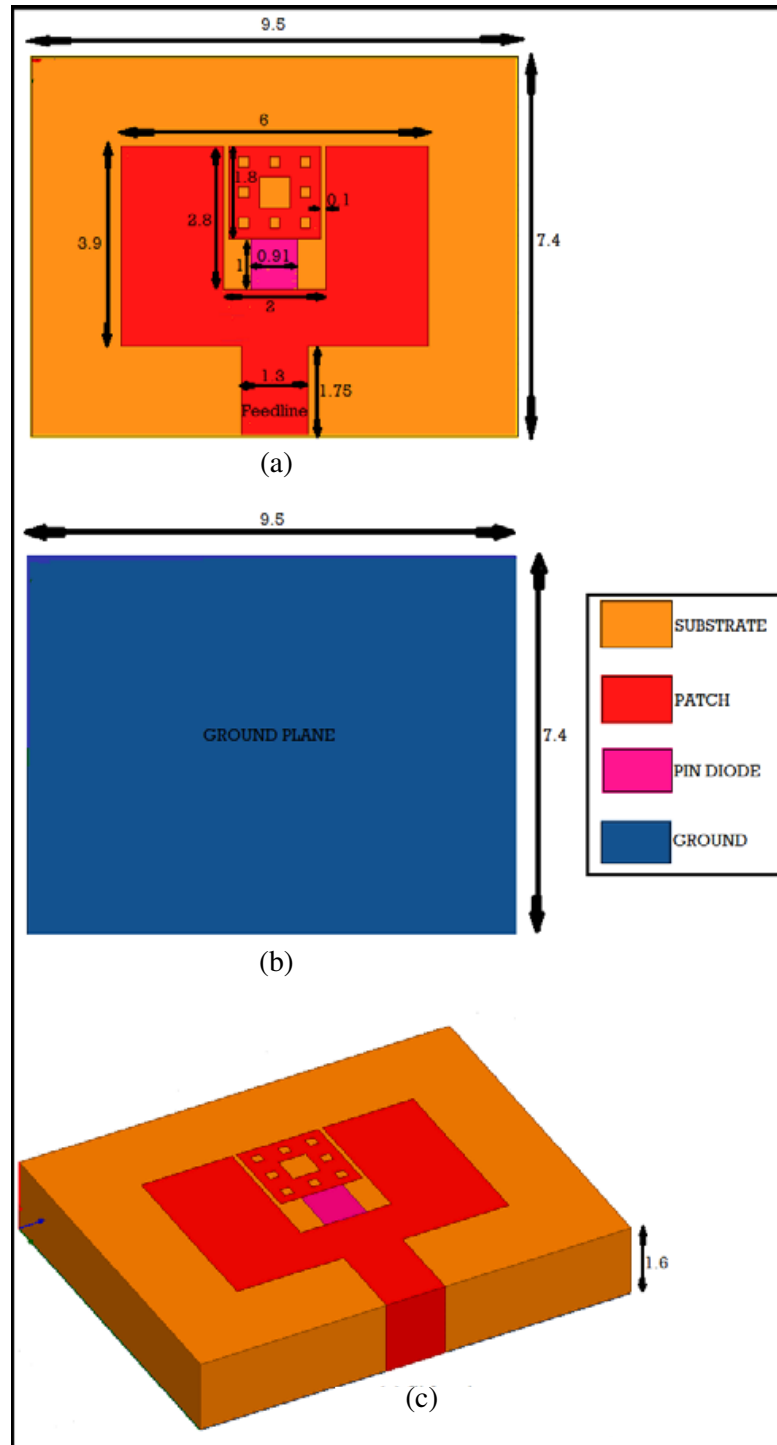


Figure 4. Proposed FRA design model. (a) Top-view. (b) Bottom-view. (c) Side-view. (All dimensions shown are in mm.).

3. RESULTS AND DISCUSSIONS

Some electrical, mechanical, and structural aspects during designing and modeling of an antenna include radiation pattern, gain, efficiency, impedance bandwidth, shape, and size. Using finite element method

solver Ansys HFSS, the proposed FRA is modeled and simulated. The proposed antenna is also fabricated and tested using Vector Network Analyzer (Agilent N5247A: A.09.90.02). The following section discusses the performance parameters obtained under the ON/OFF states of the PIN diode. PIN diodes are switching elements that are very sensitive to electrical biasing. However, owing to their ability for providing switchability and ease-of-integration with RF/microwave devices, they are widely used for antenna reconfiguration, but the cables employed for biasing and other fabrication errors tend to cause deviations in antenna measurements. The diode OFF state yields 15.24 GHz and 28.11 GHz as the resonant frequencies, and the diode ON state yields 15.15 GHz and 26.58 GHz as the resonant frequencies. It is observed that the impedance bandwidth is increased from 2.01 GHz to 3.36 GHz on switching the diode from the OFF state to the ON state. The fabricated prototype of the proposed antenna design is as shown in Fig. 5, and the antenna VNA test setup is as shown in Fig. 6. The proposed FRA is significantly miniaturized in size, becoming compact and conformable.

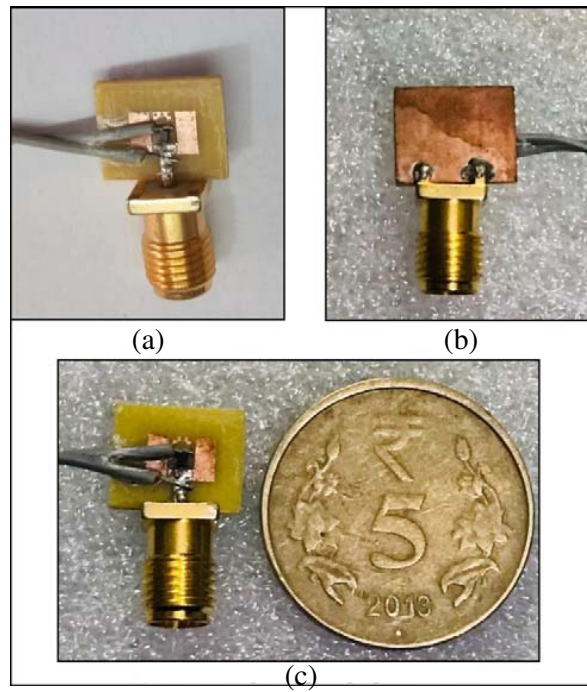


Figure 5. (a) Top-view. (b) Bottom-view. (c) Fabricated prototype of proposed FRA.

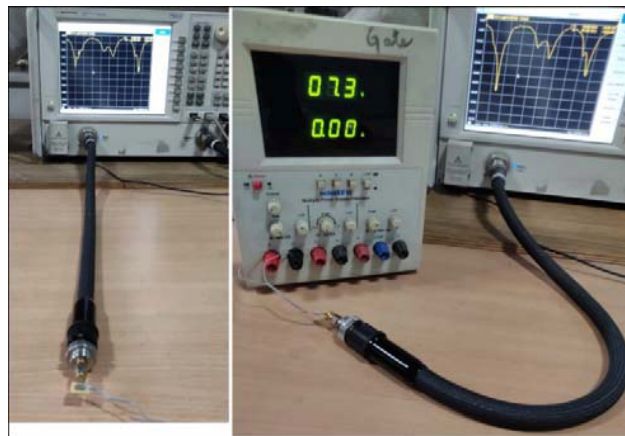


Figure 6. Antenna VNA test-setup.

3.1. Return Loss, VSWR and Impedance Bandwidth

Figures 7 and 8 show the plots of comparative analysis of simulated and measured return loss as a function of frequency for diode OFF and diode ON states, respectively. Impedance bandwidth of the

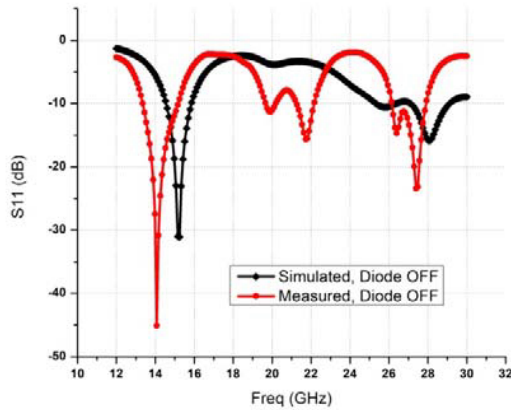


Figure 7. Return loss of proposed FRA for diode OFF state.

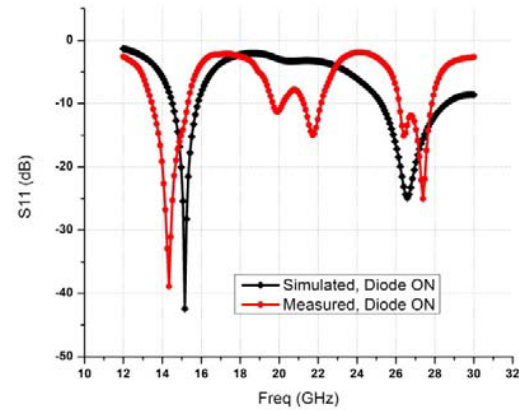


Figure 8. Return loss of proposed FRA for diode ON state.

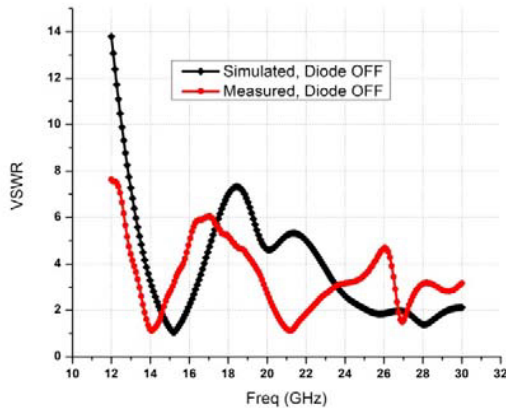


Figure 9. VSWR of proposed FRA for diode OFF state.

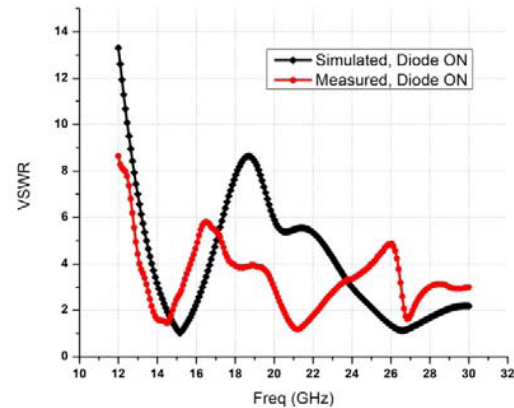


Figure 10. VSWR of proposed FRA for diode ON state.

Table 1. Return loss, VSWR and impedance bandwidth for diode off/on states.

Resonant frequency (f_r in GHz)		S_{11} (dB)	VSWR	Impedance bandwidth (GHz)
Diode OFF	15.24	-31.08	1.05	1.29 (14.56–15.85)
	28.11	-15.83	1.38	2.01 (27.11–29.12)
Diode ON	15.15	-42.44	1.01	1.3 (14.52–15.82)
	26.58	-24.90	1.12	3.36 (25.24–28.6)

antenna below -10 dB return loss has also been estimated from simulation, and it is observed that a considerable increase in bandwidth is obtained when the diode is switched from the OFF to ON state. Fig. 9 and Fig. 10 depict the comparative analysis of the simulated and measured VSWRs obtained for the two states of the diode as a function of frequency. Some variations between the simulation and measurement results exist, particularly near higher resonant frequencies, due to human error involved in the fabrication and testing process. The simulated return loss, VSWR, and impedance bandwidth are as tabulated in Table 1.

3.2. Antenna Gain, Directivity, Radiation Efficiency and Radiation Patterns

In the diode OFF state, the total gain and directivity obtained at 15.24 GHz are 6.09 dB and 6.71 dB, respectively, while those obtained at 28.11 GHz are 5.75 dB and 6.75 dB, respectively. In the diode ON state, the total gain and directivity obtained at 15.15 GHz are 6.03 dB and 6.68 dB, respectively, while those obtained at 26.58 GHz are 4.12 dB and 4.71 dB, respectively. Fig. 11 illustrates the variation of simulated peak gain in dB versus frequency for diode OFF/ON states. The plot of radiation efficiency versus frequency for diode OFF/ON states is as shown in Fig. 12. Table 2 demonstrates the simulated values of gain, directivity, and radiation efficiency for OFF/ON states of the diode. Radiation pattern describes the far-field radiations of the antenna. Fig. 13 depicts the simulated far-field radiation patterns of the proposed FRA for $\phi = 0^\circ$ and $\phi = 90^\circ$ at the resonating frequencies for the diode OFF and diode ON states, respectively. It is observed that the radiation patterns are nearly omnidirectional and stable.

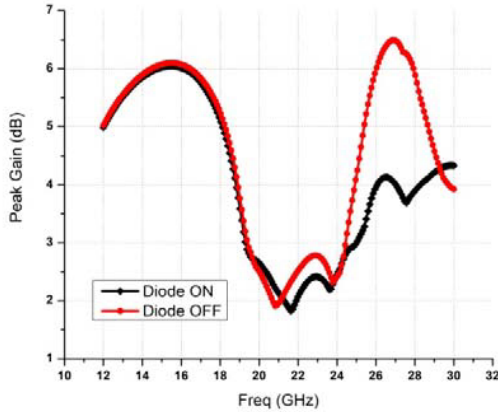


Figure 11. Peak gain (simulated) in dB for diode OFF/ON states.

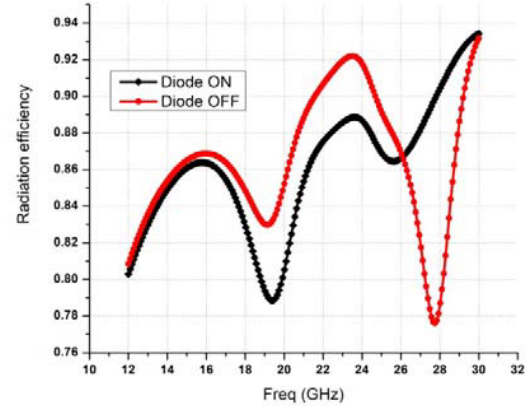


Figure 12. Radiation efficiency (simulated) for diode OFF/ON states.

Table 2. Antenna gain, directivity and radiation efficiency for diode off/on states.

Diode state (f_r in GHz)		Gain (dB)	Directivity (dB)	Radiation efficiency (%)
OFF	15.24	6.09	6.71	86.66
	28.11	5.75	6.75	79.45
ON	15.15	6.03	6.68	86.18
	26.58	4.12	4.71	87.38

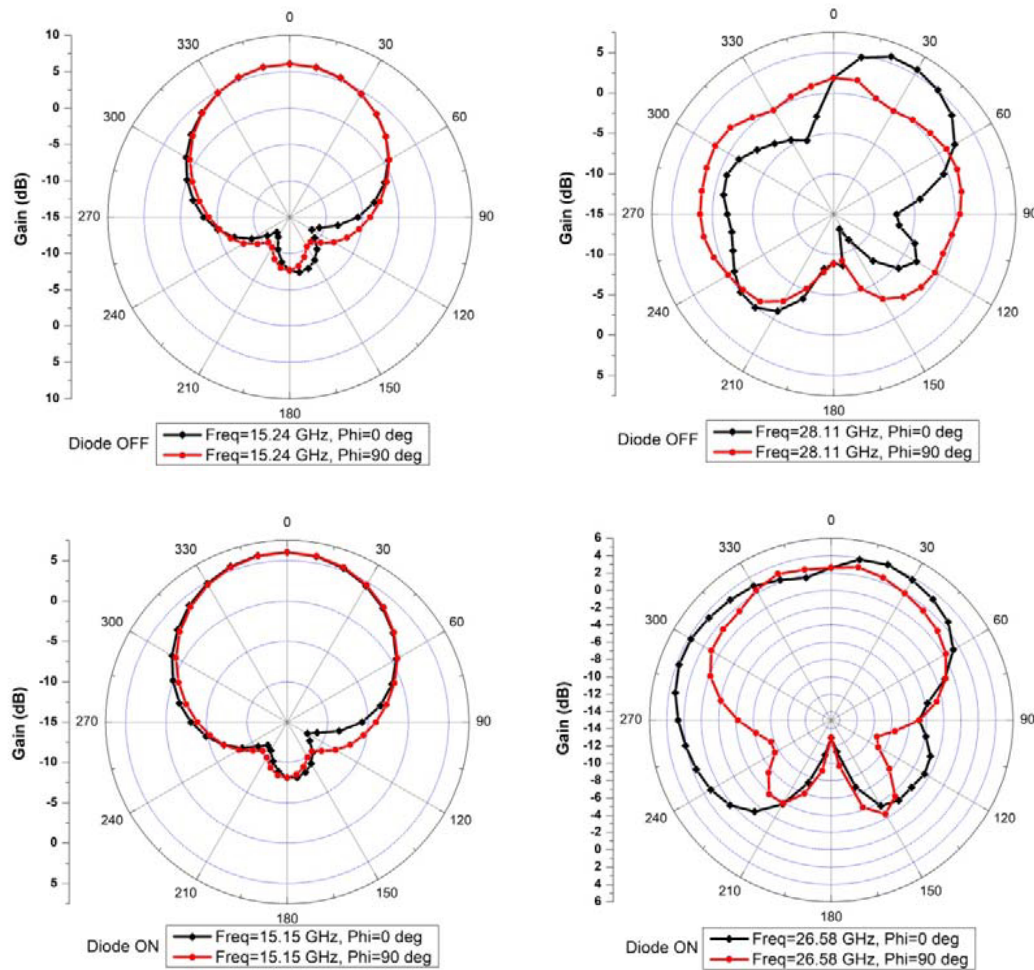


Figure 13. Proposed FRA radiation patterns (simulated) for diode OFF and diode ON states at the resonant frequencies.

3.3. Comparison of Proposed Design with Existing Designs

Proposed design has been compared with some existing designs reported in this work [11, 13, 14, 17, 18]. Table 3 depicts the comparison of the proposed antenna with existing FRAs in terms of size and highest impedance bandwidth obtained. The comparison shows that the proposed design is highly compact providing a wide impedance bandwidth.

Table 3. Comparison of proposed design with reported FRAs.

Reference	Year	Size (mm ²)	Highest Bandwidth (MHz)
[11]	2018	25.9 × 22.17	340
[13]	2016	86.3 × 50	-
[14]	2015	25.4 × 25.4	2150
[17]	2017	28 × 30	600
[18]	2019	25 × 31	1570
Proposed design	-	9.5 × 7.4	3200

4. CONCLUSION

This communication describes the fractal and reconfigurable nature of a conventional microstrip patch antenna. In this work, a Fractal Reconfigurable Antenna (FRA) is proposed that is capable of switching its frequency in the Ka band while providing a near constant resonant frequency in the Ku band. Also, a significant increase in bandwidth is obtained upon switching the diode state. The proposed antenna is capable of being used for applications in the Ku band (12–18 GHz) and Ka band (26.5–40 GHz) in the diode OFF state and Ku, Ka, and K bands (18–27 GHz) in the diode ON state. Out of these three bands, Ku band (also known as K-under band) is primarily used for satellite communication applications, and K band is employed for short-range applications while the Ka band (also known as K-above band) is targeted for radar and experimental communications.

ACKNOWLEDGMENT

The authors would like to acknowledge the University Grants Commission (UGC), India for providing financial assistance (NET JRF) to the first author (UGC-Ref. No.: 3770/(NET-DEC 2018)).

REFERENCES

1. Singh, I. and V. S. Tripathi, "Microstrip patch antenna and its applications: A survey," *International Journal of Computer Technology and Applications*, Vol. 2, 1595–1599, 2011.
2. Khanna, G. and N. Sharma, "Fractal antenna geometries: A review," *International Journal of Computer Applications*, Vol. 153, 29–32, 2016.
3. Cao, T. N. and W. J. Krzysztofik, "Design of multiband sierpinski fractal carpet antenna array for C-band," *2018 22nd International Microwave and Radar Conference (MIKON)*, 41–44, 2018.
4. Costantine, J., Y. Tawk, S. E. Barbin, and C. G. Christodoulou, "Reconfigurable antennas: Design and applications," *Proceedings of the IEEE*, Vol. 103, No. 3, 424–437, March 2015.
5. Ramadan, A., M. Husseini, K. Y. Kabalan, and A. El-Hajj, *Fractal-shaped Reconfigurable Antennas*, InTech, 2011.
6. Mohanta, H. C., A. Z. Kouzani, and S. K. Mandal, "Reconfigurable antennas and their applications," *Universal Journal of Electrical and Electronic Engineering*, Vol. 6, No. 4, 239–258, 2019.
7. Hakani, R., "A survey: Analysis of reconfigurable microstrip patch antenna," *International Journal of Innovative Research in Technology*, Vol. 1, 1029–1033, 2014.
8. Rouissi, I., J. Floch, H. Rmili, and H. Trabelsi, "Design of a frequency reconfigurable patch antenna using capacitive loading and varactor diode," *European Conference on Antennas and Propagation, EuCAP 2015*, 2015.
9. Kordzadeh, A. and F. Hojjat-Kashani, "A new reduced size microstrip patch antenna with fractal shaped defects," *Progress In Electromagnetics Research B*, Vol. 11, 29–37, 2009.
10. Chattha, H. T., M. Hanif, X. Yang, Q. H. Abbasi, and I. E. Rana, "Frequency reconfigurable patch antenna for 4G LTE applications," *Progress In Electromagnetics Research M*, Vol. 69, 1–13, 2018.
11. Kalmkar, S. and V. Bhope, "Design and analysis of frequency reconfigurable microstrip patch antenna," *International Journal of Academic Research and Development*, Vol. 3, 21–24, 2018.
12. Majid, H. A., M. K. Abdul Rahim, M. R. Hamid, N. A. Murad, and M. F. Ismail, "Frequency-reconfigurable microstrip patch-slot antenna," *IEEE Antennas and Wireless Propagation Letters*, Vol. 12, 218–220, 2013.
13. Nazir, I., I. E. Rana, N. U. A. Mir, and K. Afreen, "Design and analysis of a frequency reconfigurable microstrip patch antenna switching between four frequency bands," *Progress In Electromagnetics Research C*, Vol. 68, 179–191, 2016.
14. Sharma, B., G. Parmar, and M. Kumar, "Frequency reconfigurable microstrip patch antenna with circular slot for K-band application," *2015 International Conference on Computer, Communication and Control (IC4)*, 1–3, 2015.

15. Saravanan, M. and M. J. Rangachar, "Circular ring shaped polarization reconfigurable antenna for wireless communications," *Progress In Electromagnetics Research M*, Vol. 74, 105–113, 2018.
16. Zhang, Y., B.-Z. Wang, X.-S. Yang, and W. Wu, "A fractal Hilbert microstrip antenna with reconfigurable radiation patterns," *2005 IEEE Antennas and Propagation Society International Symposium*, Vol. 3A, 254–257, 2005.
17. Ali, T., M. M. Khaleeq, and R. C. Biradar, "A multiband reconfigurable slot antenna for wireless applications," *AEU — International Journal of Electronics and Communications*, Vol. 84, 273–280, 2017.
18. Chaouche, Y. B., M. Nedil, and I. Messaoudene, "A bandwidth reconfigurable multiband fractal antenna for wireless applications," *2019 IEEE International Symposium on Antennas and Propagation and USNC-URSI Radio Science Meeting*, 917–918, 2019.
19. Maharana, M. S., G. P. Mishra, and B. B. Mangaraj, "Design and simulation of a Sierpinski carpet fractal antenna for 5G commercial applications," *2017 International Conference on Wireless Communications, Signal Processing and Networking (WiSPNET)*, 1718–1721, 2017.
20. Ramadan, A., M. Al-Husseini, K. Y. Kabalan, A. El-Hajj, and J. Costantine, "A compact Sierpinski-carpet-based patch antenna for UWB applications," *2009 IEEE Antennas and Propagation Society International Symposium*, 1–4, 2009.
21. Balanis, C. A., *Antenna Theory, Analysis and Design*, John Wiley and Sons, 2005.
22. Duvall, P., J. Keesling, and A. Vince, "The Hausdorff dimension of the boundary of a self-similar tile," *Journal of the London Mathematical Society*, Vol. 61, 1999.
23. Rahim, M. K. A., N. Abdullah, and M. Z. A. Abdul Aziz, "Microstrip Sierpinski carpet antenna design," *2005 Asia-Pacific Conference on Applied Electromagnetics*, 4, 2005.
24. Singh, R. K., A. Basu, and S. K. Koul, "Reconfigurable microstrip patch antenna with polarization switching in three switchable frequency bands," *IEEE Access*, Vol. 8, 119376–119386, 2020.
25. <https://cdn.macom.com/datasheets/MA4SPS402.pdf>.
26. Garg, R., P. Bhartia, I. Bahl, and A. Ittipiboon, *Microstrip Antenna Design Handbook*, Artech House, Boston, London, 2003.
27. Ansari, J., N. P. Yadav, P. Singh, and A. Mishra, "Compact half U-slot loaded shorted rectangular patch antenna for broadband operation," *Progress In Electromagnetics Research M*, Vol. 9, 215–226, 2009.
28. Siddiqui, M. G., A. K. Saroj, Devesh, and J. Ansari, "Multi-band fractaled triangular microstrip antenna for wireless applications," *Progress In Electromagnetics Research M*, Vol. 65, 51–60, 2018.